PHYSICAL REVIEW D **88,** 044009 (2013)

Non-singular quantum-inspired gravitational collapse

Cosimo Bambi,* Daniele Malafarina,† and Leonardo Modesto‡

Department of Physics, Center for Field Theory and Particle Physics, Fudan University, 200433 Shanghai, China

(Received 23 May 2013; published 5 August 2013)

We consider general relativistic homogeneous gravitational collapses for dust and radiation. We show that replacing the density profile with an effective density justified by some quantum gravity framework leads to the avoidance of the final singularity. The effective density acts on the collapsing cloud by introducing an isotropic pressure, which is negligible at the beginning of the collapse and becomes negative and dominant in the strong-field regime. Event horizons never form and therefore the outcome of the collapse is not a black hole, in the sense that there are no regions causally disconnected from future null infinity. Apparent horizons form when the mass of the object exceeds a critical value, disappear when the matter density approaches an upper bound and gravity becomes very weak (asymptotic-freedom regime), form again after the bounce as a consequence of the decrease in the matter density, and eventually disappear when the density becomes too low and the matter is radiated away. The possibility of detecting radiation coming from the high-density region of a collapsing astrophysical object in which classically there would be the creation of a singularity could open a new window to experimentally test theories of quantum gravity.

DOI: 10.1103/PhysRevD.88.044009 PACS numbers: 04.20.Dw, 04.20.Jb, 04.70.Bw, 04.60.Bc

I. INTRODUCTION

The search for a theory of quantum gravity is surely one of the most important open issues in contemporary theoretical high energy physics and a very active research field. The key problem is the complete absence of experimental data capable of testing the validity of the large number of different models that have been proposed so far. Up to now, we have no observational evidence of any quantum gravity phenomenon. The natural energy scale of quantum gravity is the Planck mass $M_{\rm Pl} \sim 10^{19}$ GeV, which is definitively too high to be reached in particle colliders on Earth, even in the foreseeable future.

In the literature, there are a few proposals that try to catch observational signatures of quantum gravity effects. The most promising approach is likely the study of some primordial features in the cosmic microwave background radiation; they are supposed to have been generated during inflation and may encode some details about quantum gravity [1]. Another proposal concerns the possibility of the existence of large extra dimensions; in these models, gravity could become strong at energies much lower than $M_{\rm Pl}$, and possibly accessible in future colliders [2]. However, these scenarios encounter serious problems when they have to explain the cosmology of the early Universe. A third idea is to detect photons from very distant sources and check if there is a delay in the arrival time of photons with different energies, as a consequence of Planck-scale-suppressed corrections to the standard dispersion relation [3]. It is not really clear if this is actually a test of quantum gravity or of the structure of the spacetime, and as of now all the data are consistent with the normal dispersion relation of special relativity.

This paper is the first study of a program whose aim is to investigate the possibility of observing quantum gravity-related phenomena in the gravitational collapse of very massive stars. General relativistic equations for gravitational collapse can describe the final stages of the life of a star when its dense core implodes under its own gravity. In the standard picture, if the neutron degeneracy pressure threshold is passed, there is nothing capable of halting the collapse, and the final product is a spacetime singularity, where the matter density diverges, predictability is lost, and standard physics breaks down. Depending on the formation of trapped surfaces, the singularity may either be hidden behind a horizon—and in this case the outcome of the collapse would be a black hole—or be naked, and thus be visible to distant observers. The weak cosmic censorship conjecture asserts that singularities formed from gravitational collapse must be hidden within black holes [4]. Although some examples are known in which naked singularities can form from regular initial data, their stability and genericity are not well understood at present; see, e.g., Ref. [5] for some early results, and Ref. [6] for a recent review. We know that a black hole in which the central singularity is replaced by a finite distribution of exotic matter can in principle lose its horizon [7], a result that suggests how the behavior of matter fields in the last stages of collapse is important for the horizon structure and hints toward a possible resolution of the central singularity. For some references on the possibility of observationally testing the existence of singularities, see, e.g., Ref. [8] and references therein. For all these reasons, it has now become of crucial importance to understand if we can

*bambi@fudan.edu.cn
†daniele@fudan.edu.cn
‡lmodesto@fudan.edu.cn

observationally test the strong-field regime where the classical relativistic framework might fail. Our strategy is to investigate how quantum effects can affect the formation of the singularity and of the trapped surfaces in order to see if the properties of the radiation emitted during the collapse in the ultra-dense region close to the classical singularity can reach distant observers and possibly carry information about the quantum gravity regime.

If we understand the singularity as a regime where the classical description breaks down and Planck-scale effects arise, then the classical formation of a naked singularity suggests that these effects might propagate and influence the outside universe. The singularity would presumably be resolved within a theory of quantum gravity [9,10] and the existence of solutions where the classical singularity is naked would then indicate that spacetime regions of extremely high density occurring at the core of the collapse might be causally connected to the outside universe, thus bringing hints of new physics from catastrophic astrophysical events. Since we do not yet have any theory of quantum gravity, most attempts reduce to the study of some effective theory that describes quantum gravity at a semiclassical level by the introduction of an appropriate modification of Einstein gravity in the strong-field regime. Attempts to reformulate classical models within a quantum gravity approach have been successfully applied to cosmology [11], where the big bang singularity can be resolved and replaced by a bounce. In the context of gravitational collapse, loop quantum gravity (LQG) has been used to show how the singularity appearing at the end of the collapse can be removed [12]. It can be shown that quantum corrections to Einstein's equations can be put in a semiclassical framework where effective quantities take the place of the classical ones. Such an approach was used in Ref. [13], where LQG corrections to the collapse of a scalar field were considered. Here, we will implement a similar strategy for the collapse of both a cloud of non interacting particles (dust) and a perfect fluid with a linear equation of state that describes radiation. The treatment is completely classical and the quantum corrections appear in the form taken by the effective density and effective pressure of the system.

The Oppenheimer-Snyder (OS) marginally bound collapse of a dust sphere is the simplest case of gravitational collapse [14]. Although the model is extremely simple, it can give some insights into the behavior of classical gravity in the strong-field regime. In this model, the singularity that forms at the end of the collapse is always hidden behind a horizon. It is known that the introduction of pressures in dust collapse can halt the process and cause a bounce. In the classical picture, in order to have a physically viable model, the pressure profile must satisfy certain assumptions, like the weak energy condition. On the other hand, we can study the case of collapse with pressures that lead to a bounce, neglecting the weak energy condition, if we are willing to reinterpret the "exotic" matter content on the right-hand side of Einstein's equations as a semiclassical limit coming from an effective theory of quantum gravity inducing corrections in the small-scale/strong-gravity regime.

In this scenario, there is a new scale introduced in the evolution. It is governed by the value of the classical critical density $\rho_{\rm cr}$, which is a parameter *a posteriori* related to the Planck-scale regime to be introduced from external considerations (such as LQG) and we can retrieve the classical solution in the limit of $\rho_{\rm cr}$ going to infinity. In our simplest quantum-gravity-inspired gravitational collapse, the physical matter density reaches its maximum value $\rho_{\rm cr}$ at the critical time $t_{\rm cr} < t_{\rm s}$, where $t_{\rm s}$ is the time at which the singularity was reached in the classical case. At $t_{\rm cr}$, the gravitational force is turned off (the effective density vanishes) and we are in a regime of asymptotic freedom. At this time, we have a bounce and the collapsing object starts expanding. As we consider the simplest case of homogeneous density and pressure, at the bounce the gravitational force is switched off everywhere and there is no apparent horizon. The latter forms again after the bounce and eventually disappears forever. So, an event horizon never forms, in the sense that there are no regions causally disconnected from future null infinity. The collapse cannot form a black hole, but only a temporary apparent horizon that can mimic a black hole for a time much shorter than the whole process of collapse and expansion.

The paper is organized as follows. In Sec. II, we briefly summarize the classical framework for relativistic collapse: in Sec. II A, we review the basic equations of the OS homogeneous dust model, while Sec. II B is for the Friedmann-Robertson-Walker (FRW) radiation collapse model. In Sec. III, we present our quantum-inspired gravitational collapse toy model and we show how the effective density coming from quantum corrections can resolve the formation of the singularity. Finally, Sec. IV is devoted to a brief summary and future perspectives.

II. GRAVITATIONAL COLLAPSE

The most general spherically symmetric metric describing a collapsing cloud of matter in comoving coordinates is given by

$$ds^2 = -e^{2\nu}dt^2 + \frac{R'^2}{G}dr^2 + R^2 d\Omega^2, \tag{1}$$

where $d\Omega^2$ represents the line element on the unit two-sphere and ν, R, and G are functions of t and r. The energy-momentum tensor is given by

$$T^{\mu}_{\nu} = \mathrm{diag}\{\rho(r,t), p_r(r,t), p_\theta(r,t), p_\theta(r,t)\}, \tag{2}$$

and Einstein's equations relate the metric functions to the matter content,

$$p_r = -\frac{\dot{F}}{R^2\dot{R}}, \tag{3}$$

$$\rho = \frac{F'}{R^2R'}, \tag{4}$$

$$\nu' = 2\frac{p_\theta - p_r}{\rho + p_r}\frac{R'}{R} - \frac{p_r'}{\rho + p_r}, \tag{5}$$

$$\dot{G} = 2\frac{\nu'}{R'}\dot{R}G, \tag{6}$$

where the $'$ denotes a derivative with respect to r, and the $\dot{}$ denotes a derivative with respect to t. The function $F(r, t)$, which is proportional to the amount of matter enclosed within the shell labeled by r at the time t, is called the Misner-Sharp mass, and is given by

$$F = R(1 - G + e^{-2\nu}\dot{R}^2). \tag{7}$$

The whole system has a gauge degree of freedom that can be fixed by setting the scale at a certain time. In the case of collapse, the usual prescription is that the area radius $R(r, t)$ is set equal to the comoving radius r at the initial time $t_i = 0$, $R(r, 0) = r$. We can then introduce a scale function a,

$$R(r, t) = ra(r, t), \tag{8}$$

that will go from 1, at the initial time, to 0, at the time of the formation of the singularity. The condition to describe collapse is thus given by $\dot{a} < 0$. The regularity of the energy density at the initial time, as seen from Eq. (4), requires that $F(r, t) = r^3M(r, t)$, with $M(r, t) = \sum_{n=0}^{\infty} M_n r^n$.

In order to have a physically realistic collapse, one typically requires some conditions for the matter model. Usually the assumptions are the following.

(1) The regularity of the initial data for density and pressure.
(2) The absence of cusps at the center for the energy density [which implies that $M'(0, t) = 0$].
(3) The energy density does not increase from the center outwards at any given time.
(4) The weak energy condition ($\rho \geq 0$, $\rho + p_r \geq 0$, and $\rho + p_\theta \geq 0$).

We know that the energy conditions are averaged classical inequalities that do not take into consideration the microscopic properties of the matter and are likely to be violated in the semiclassical quantum regime [15].

A. Classical dust model

Let us now consider the simplest case of dust collapse, known as Lemaître-Tolman-Bondi model, where $p_r = p_\theta = 0$ [16]. In the Lemaître-Tolman-Bondi model, from Eq. (3) one immediately gets that $M = M(r)$ and the cloud can be matched to a Schwarzschild exterior with total mass $2M_T = F(r_b)$ at the boundary r_b [17]. From Eq. (5), one can choose the time gauge in such a way that $\nu = 0$. Then Eq. (6) implies $G = 1 + f(r)$, which in the marginally bound case (representing particles that fall from infinity with zero initial velocity) simply becomes $G = 1$. The metric is then given by

$$ds^2 = -dt^2 + R'^2dr^2 + R^2d\Omega^2. \tag{9}$$

The Misner-Sharp mass, Eq. (7), takes the form of an equation of motion,

$$\dot{a} = -\sqrt{\frac{M}{a}}, \tag{10}$$

with the minus sign chosen in order to describe a collapse. The integration of Eq. (10) is straightforward and gives

$$a(r, t) = \left(1 - \frac{3}{2}\sqrt{M}t\right)^{2/3}. \tag{11}$$

Then the remaining Einstein's equation, Eq. (4), is written as

$$\rho = \frac{3M + rM'}{a^2(a + ra')}, \tag{12}$$

which completely solves the system.

The model has a strong-curvature singularity for $a \to 0$, as can be seen from the divergence of the Kretschmann scalar,

$$R_{\mu\nu\rho\sigma}R^{\mu\nu\rho\sigma} = 12\frac{\ddot{a}^2a^2 + \dot{a}^4}{a^4}. \tag{13}$$

The singularity is achieved along the curve $t_s(r) = 2/3\sqrt{M}$ and the central line $r = 0$ is regular for $a \neq 0$. The central singularity $t_s(0)$ can be visible to faraway observers depending on the matter profile $M(r)$ [18]. In the present work, we restrict our attention to the simplest case, the OS dust collapse, where the choice of $M(r) = M_0$ causes the density to be homogeneous and the final outcome is a black hole. In the OS model, the metric takes the form

$$ds^2 = -dt^2 + a^2(dr^2 + r^2d\Omega^2), \tag{14}$$

which is the time reversal of the FRW cosmological scenario. We then get

$$\rho(t) = \frac{3M_0}{a^3}, \tag{15}$$

$$M_0 = a\dot{a}^2, \tag{16}$$

$$a(t) = \left(1 - \frac{3}{2}\sqrt{M_0}t\right)^{2/3}, \tag{17}$$

and all the shells become singular at the same comoving time $t_s = 2/3\sqrt{M_0}$. Here, the apparent horizon forms at the boundary at a time antecedent to the formation of the singularity, thus leaving the region where Planck-scale effects arise hidden from faraway observers.

B. Classical radiation model

We turn now to the classical FRW solution describing the collapse of a homogeneous perfect fluid, where $p_r = p_\theta = p(t)$, and consider the case of radiation where the equation of state relating the pressure to the density is

$$\rho = 3p. \tag{18}$$

The isotropy and homogeneity of the pressure implies that Eq. (6) must give $G = 1 + f(r)$, in analogy with the dust case. Again, we will consider here the marginally bound solution with $f = 0$. Unlike in the dust scenario, the presence of the homogeneous pressure indicates that the mass profile is not constant throughout the collapse, i.e., M must depend on t, and therefore the matching with the exterior must be done with the Vaidya solution [19]. The equation of state together with Einstein's equations (3) and (4) implies that the mass profile must satisfy the following differential equation:

$$\frac{dM}{da} = -\frac{M}{a}, \tag{19}$$

which gives $M = \frac{M_0}{a}$. Then the energy density becomes

$$\rho = \frac{3M_0}{a^4} \tag{20}$$

and

$$M_0 = a^2\dot{a}^2. \tag{21}$$

Finally, the integration of the equation of motion (10) gives

$$a(t) = (1 - 2\sqrt{M_0}t)^{1/2}. \tag{22}$$

Once again, the metric is given by Eq. (14), and the singularity occurs at the same time $t_s = 1/2\sqrt{M_0}$ for each shell. Like in the dust model, the final outcome is a black hole.

III. QUANTUM-INSPIRED COLLAPSE

The above system of Einstein's equations for dust or radiation collapse is closed once a free function is specified—typically the mass profile M or the density profile ρ. In the case of the OS model, we have chosen the mass profile $M = M_0$, while for the radiation model we have specified the equation of state (18). Therefore an effective model of quantum gravitational collapse can be given by a well-motivated choice of the free function that replaces the classical choice, while introducing a scale factor in the form of a critical density $\rho_{\rm cr}$ that can be related to the Planck scale. We can then interpret the model as a modification to the standard dust or radiation collapse scenario induced by quantum corrections in the strong-field limit. To this aim, we can rewrite the right-hand side of Einstein's equations as dust + corrections or radiation + corrections, and the newly introduced parameter $\rho_{\rm cr}$ indicates the scale at which the corrections become relevant. Typically, we will have the correction becoming important at high densities, so one can write

$$\rho_{\rm corr} = \alpha_1\rho^2 + \alpha_2\rho^3 + o(\rho^3), \tag{23}$$

where the parameters $\alpha_i = \alpha_i(\rho_{\rm cr})$ that determine the scale of the quantum corrections will go as an inverse power of $\rho_{\rm cr}$ and in general will be determined from the quantum theory. In this way, we can write $T_{\mu\nu} = T^{\rm class}_{\mu\nu} + T^{\rm corr}_{\mu\nu}$, where, for dust, we obviously have $p_{\rm class} = 0$. We can then move the correction $T^{\rm corr}_{\mu\nu}$ to the left-hand side of Einstein's equations, thus reinterpreting the model as a dust or radiation solution in some effective theory of gravity that accounts for corrections in the strong-field limit. This procedure is completely equivalent to replacing Newton's constant for classical gravity $G_{\rm N}$ with a variable coupling function $G(\rho)$ derived from the effective quantum theory.

We expect that quantum effects become relevant towards the formation of the singularity, as they are supposed to "smear" the singularity, thus avoiding the breakdown of predictability that occurs in the classical case. In general, the system of Einstein's equations for perfect fluid collapse, when the equation of state is not specified, leaves the freedom to choose one free function. It is not difficult to show that a suitable choice of the mass profile can drastically change the structure underlying the formation of the horizon and singularity (see, for example, Ref. [20]). In order to study how the inclusion of quantum effects in the form of an effective theory affects the formation of the singularity at the end of the collapse, we assume that at first order the corrections due to quantum gravity take the form given by Eq. (23) and thus we guess an effective energy density profile as a function of the dust and radiation energy densities [as written in Eqs. (15) and (20), respectively] as $\rho_{\rm eff} = \rho + \rho_{\rm corr}$ and take this as the free function for the system.

Following Ref. [13], we consider here an effective theory of gravity where the corrections to the energy density (23) take the form

$$\rho_{\rm eff} = \rho\left(1 - \frac{\rho}{\rho_{\rm cr}}\right)^\gamma, \qquad \gamma \geq 1, \tag{24}$$

and the effective density specified by this equation will play the role of the free function in the effective model for collapse. In the following, we will consider the cases $\gamma = 1$ and 2. The case $\gamma = 1$ corresponds to the choice of $\alpha_1 = -1/\rho_{\rm cr}$ and $\alpha_i = 0$ for $i > 1$. The case $\gamma = 2$ corresponds to the choices $\alpha_1 = -2/\rho_{\rm cr}$, $\alpha_2 = 1/\rho^2_{\rm cr}$, and $\alpha_i = 0$ for $i > 2$. In the weak-field limit, for large $\rho_{\rm cr}$, quantum corrections become negligible, and in the limit of infinite $\rho_{\rm cr}$ we recover the classical dust and radiation cases. For low densities (i.e., close to the initial time), the effective energy density approaches that of the classical models.

A. Quantum-inspired dust model

Let us note that the scale function a that appears in Eq. (15) must now be determined from the integration of the new equation of motion coming from Eq. (23) that replaces Eq. (16). This now becomes

$$\dot{a}^2 = \frac{M_0}{a} + \alpha_1 \frac{3M_0^2}{a^4} + \alpha_2 \frac{9M_0^3}{a^7} + \cdots. \tag{25}$$

Here, we will consider an effective density of the form given in Eq. (24), as suggested by first-order corrections coming from LQG, and integrate for the cases $\gamma = 1$ and 2. We then proceed to solve Einstein's equations for the effective theory where the density ρ, the pressure p, and the Misner-Sharp mass M are replaced by the corresponding effective quantities (namely $\rho_{\rm eff}$, $p_{\rm eff}$, and $M_{\rm eff}$). Equation (15) then becomes

$$\rho_{\rm eff} = \frac{3M_{\rm eff}}{a^3}, \tag{26}$$

where the new effective mass $M_{\rm eff}(t)$ is again given by $M_{\rm eff}(t) = a\dot{a}^2$ and is not constant (the fact that $M_{\rm eff}$ is a function of t induces the presence of the effective pressure $p_{\rm eff}$). We then obtain the differential equation for the scale function $a(t)$ from Eqs. (24) and (26),

$$\dot{a}^2 = \frac{M_0}{a^{3\gamma+1}}(a^3 - a_{\rm cr}^3)^\gamma, \quad \text{with} \quad a_{\rm cr}^3 = \frac{3M_0}{\rho_{\rm cr}}, \tag{27}$$

where we have introduced the critical scale $a_{\rm cr}$. Let us note that, for $a_{\rm cr} \to 0$, we recover the dust solution with $\rho_{\rm eff} = \rho$ and $a(t)$ given by Eq. (17). Once solved with the initial condition $a(1) = 1$, Eq. (27) gives

$$t(a) = \frac{2}{3\sqrt{M_0}}\left(\sqrt{1 - a_{\rm cr}^3} - \sqrt{a^3 - a_{\rm cr}^3}\right) \quad \text{for } \gamma = 1, \tag{28}$$

$$t(a) = \frac{2}{3\sqrt{M_0}}(1 - a^{3/2}) - \frac{a_{\rm cr}^{3/2}}{3\sqrt{M_0}} \ln \frac{(a^{3/2} - a_{\rm cr}^{3/2})(1 + a_{\rm cr}^{3/2})}{(a^{3/2} + a_{\rm cr}^{3/2})(1 - a_{\rm cr}^{3/2})} \quad \text{for } \gamma = 2. \tag{29}$$

The metric for the effective model is still described by the usual form given by Eq. (14).

The effective energy density for the toy model studied here is homogeneous. This causes the effective dynamics of the system to be equivalent to that of the collapse of a homogeneous perfect fluid where the pressure, coming from Einstein's equation (3), is given by

$$p_{\rm eff}(t) = -\frac{\dot{M}_{\rm eff}}{a^2\dot{a}}. \tag{30}$$

The effective pressure that describes the quantum corrections in the semiclassical theory is then homogeneous as well. From

$$M_{\rm eff} = M_0\left(1 - \frac{\rho}{\rho_{\rm cr}}\right)^\gamma, \tag{31}$$

we see that the effective pressure becomes

$$p_{\rm eff} = -\gamma\frac{\rho^2}{\rho_{\rm cr}}\left(1 - \frac{\rho}{\rho_{\rm cr}}\right)^{\gamma-1}. \tag{32}$$

The effective pressure is always negative and, in the case $\gamma = 1$, approaches the limiting case of $p = -\rho$ as the density approaches $\rho_{\rm cr}$. On the other hand, in the case $\gamma > 1$, the pressure goes to zero as $\rho \to \rho_{\rm cr}$ (as expected, it becomes zero in the limit of $\rho_{\rm cr}$ going to infinity). The fact that the effective pressure becomes negative in the strong-field regime is what causes the bounce of the new density. At the initial time, the new density is equal to the density in the classical case, while the effective pressure is very small, although not zero (being zero in the limit of $\rho_{\rm cr}$ going to infinity). From these considerations, it is easy to verify that the weak energy condition is satisfied at the beginning of collapse, and it is violated as the quantum gravity regime is approached.

It is worth noting that the scale function $a(t)$ behaves differently for the models with $\gamma = 1$ and $\gamma = 2$. In the first case, a reaches the minimum value $a_{\rm cr}$ in a finite time $t_{\rm cr}$, and then grows indefinitely, thus originating a gravitational bounce. On the other hand, in the case $\gamma = 2$, the minimum at $a_{\rm cr}$ is reached only as $t \to \infty$ and therefore there is no bounce but an indefinite collapse that slows down until it stops asymptotically (see the right panel in Fig. 1). The different behavior of a for different values of γ is also reflected in a different behavior for the apparent horizon. In the case $\gamma = 1$ the apparent horizon curve $r_{\rm ah}(t)$ diverges for t approaching $t_{\rm cr}$, while in the case $\gamma = 2$ it diverges for $t \to \infty$.

We will now concentrate on the case $\gamma = 1$. The scale function has the form

$$a(t) = \left[a_{\rm cr}^3 + \left(\sqrt{1 - a_{\rm cr}^3} - \frac{3\sqrt{M_0}}{2}t\right)^2\right]^{1/3}, \tag{33}$$

and it reaches a minimum at the time

$$t_{\rm cr} = \frac{2\sqrt{1 - a_{\rm cr}^3}}{3\sqrt{M_0}} < t_{\rm s}, \tag{34}$$

at which $\rho_{\rm eff}$ vanishes, and then increases for $t > t_{\rm cr}$ (see the right panel in Fig. 1). The fact that the time of the bounce $t_{\rm cr}$ occurs before the classical time of the singularity is due to the choice of the integration constant in Eq. (33), which for collapse is chosen in order to have $a(0) = 1$. In standard cosmological models, the constant is chosen in such a way that $t_{\rm s} = t_{\rm cr}$ and leads to an initial condition $a^3(0) = 1 + a_{\rm cr}^3 > 1$ for the effective model. Of course, the metric is invariant under time translations, so the crucial point here is that once an initial time $t_{\rm i}$ is fixed in such a way that the metric coefficients take the same

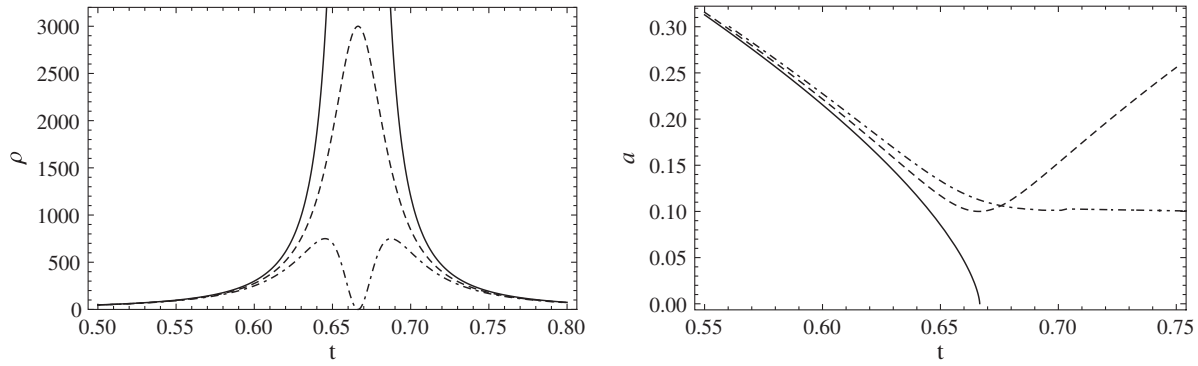

FIG. 1. Dust collapse models. Left panel: The density ρ in the classical model (solid line), the density ρ in the quantum-gravity-inspired collapse model with $\gamma = 1$ (dashed line), and the effective density $\rho_{\rm eff}$ in the quantum-gravity-inspired collapse model with $\gamma = 1$ (dashed-dotted line). Right panel: Plot of $a(t)$ in the classical case (solid line) and in the semiclassical model with $\gamma = 1$ (dashed line) and $\gamma = 2$ (dotted-dashed line). Near the initial time, the semiclassical model has a behavior close to the dust. a either reaches a minimum at $t = t_{\rm cr}$ and then grows for $t > t_{\rm cr}$ ($\gamma = 1$), or approaches asymptotically a minimum value ($\gamma = 2$). Here, $M_0 = 1$ and $\rho_{\rm cr} = 3000$. See the text for details.

numerical values in the classical and quantum case then the interval $\Delta t_{\rm s} = |t_{\rm s} - t_{\rm i}|$ is greater than the interval $\Delta t_{\rm cr} = |t_{\rm cr} - t_{\rm i}|$. The effective density reaches a maximum at the time $t_{\rm max} = t_{\rm s}(\sqrt{1 - a_{\rm cr}^3} - \sqrt{a_{\rm cr}^3})$ and then decreases, becoming zero at the critical time $t_{\rm cr}$.

Contrary to the classical dust case, where ρ diverges at the time $t_{\rm s} = 2/3\sqrt{M_0}$, in our case we can see that the new density $\rho = 3M_0/a^3$ tends to the maximum value $\rho_{\rm cr}$ as t goes to $t_{\rm cr}$ and then decreases (see the left panel in Fig. 1). Also, the velocity of the collapsing shells $\dot{a}$ tends to zero as t goes to $t_{\rm cr}$, unlike the classical case where the velocity is finite at $t_{\rm cr}$ and diverges when we approach the singularity.

In this model, the strong-curvature singularity is removed: the Kretschmann scalar is still given by Eq. (15), but with the new scale function a it never diverges. Furthermore, the fact that we are dealing with a homogeneous perfect fluid for which the area radius is $R(r, t) = ra(t)$, together with the positivity of the scale function a, ensures that there are no shell-crossing singularities in the spacetime, which is therefore everywhere regular until $t = t_{\rm cr}$ and can be prolonged for $t > t_{\rm cr}$. The effective mass of the collapsing perfect fluid cloud is given by Eq. (31). We can see that $M_{\rm eff}$ decreases, becoming zero in the limit of t going to $t_{\rm cr}$ (see the left panel in Fig. 2). Therefore the matching with the exterior spacetime must be done with the Vaidya solution describing outgoing radiation. Further, from the fact that $\rho_{\rm eff}(t_{\rm cr}) = M_{\rm eff}(t_{\rm cr}) = 0$, at $t = t_{\rm cr}$ the spacetime is flat. This happens because in our model gravity becomes weaker and weaker as ρ approaches $\rho_{\rm cr}$ and is turned off when $\rho = \rho_{\rm cr}$. The bounce occurs at $t = t_{\rm cr}$ and then the collapse changes into an expansion. At lower densities, we recover Einstein's gravity, but now the model describes an expanding cloud with $\dot{a} > 0$.

The collapsing matter is usually required to satisfy the weak energy condition, which in the case of a perfect fluid reads $\rho + p \geq 0$. For the effective theory described here, it is easy to check that $\rho_{\rm eff} + p_{\rm eff} \geq 0$ is satisfied in the

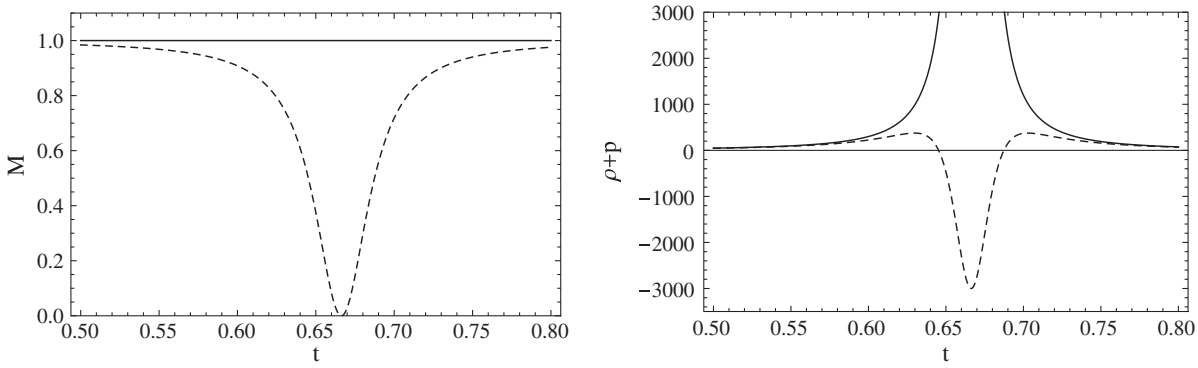

FIG. 2. Dust collapse models. Left panel: The mass profile $M = M_0$ (solid line) and $M_{\rm eff}$ for $\gamma = 1$ (dashed line). At $t = t_{\rm cr}$, the effective mass vanishes and thus the spacetime is flat; we are in a regime of asymptotic freedom. Right panel: In order to investigate the breakdown of the weak energy condition, we plot ρ for the classical dust case (solid line) and $\rho_{\rm eff} + p_{\rm eff}$ for $\gamma = 1$ (dashed line). Here, $M_0 = 1$ and $\rho_{\rm cr} = 3000$. See the text for details.

weak-field regime, close to the initial time, while it is violated due to the negative pressures as we approach the critical density ρ_{cr} (see the right panel in Fig. 2).

In general relativity, under common assumptions like matter-energy conditions and cosmic censorship, the appearance of an apparent horizon is related to the existence of an event horizon. This is not the case here, because of the unconventional properties of our effective matter. Despite that, it is convenient to study the apparent horizon of the spacetime and to compare the results with the scenario of the standard picture. The condition for the formation of trapped surfaces is given by the requirement that the surface $R(r, t) = \text{const}$ is null; that is, $g^{\mu\nu}(\partial_\mu R)(\partial_\nu R) = 0$. For the metric in Eq. (1), this means

$$G - e^{-2\nu}\dot{R}^2 = 0, \tag{35}$$

and, from the definition of the Misner-Sharp mass (7), we can write it as

$$1 - \frac{F}{R} = 0. \tag{36}$$

In the dust case, the condition for the absence of trapped surfaces at the initial time reduces to $r^2 M_0 < 1$, while in the model presented here we must require $r^2 M_0 \sqrt{1 - a_{cr}^3} < 1$. In the classical OS case, the apparent-horizon curve is given by

$$t_{ah}(r) = t_s - \frac{2}{3} r^3 M_0. \tag{37}$$

In our model, the central singularity is avoided. What happens to the formation of trapped surfaces? The equation for the apparent horizon becomes

$$r_{ah}(t) = \frac{a^2}{\sqrt{M_0(a^3 - a_{cr}^3)}}. \tag{38}$$

It is not difficult to check that r_{ah} has a minimum for

$$t = t_{min} = t_s\left(\sqrt{1 - a_{cr}^3} - \sqrt{3a_{cr}^3}\right). \tag{39}$$

Therefore there exists a minimum radius

$$r_{min} = r_{ah}(t_{min}) = 2^{4/3}\sqrt{\frac{a_{cr}}{3M_0}}, \tag{40}$$

for which, if the boundary is taken as $r_b < r_{min}$, no trapped surfaces form during the whole process of collapse and bounce (see Fig. 3).

The existence of a minimum radius implies that in the quantum-modified scenario there exists a minimal mass M_{min} below which an apparent horizon never forms. In fact, considering the boundary condition for dust collapse $2M_T = r_b^3 M_0$, where M_T is the total mass in the exterior spacetime, if we take the boundary $r_b = r_{min}$, we can evaluate M_{min} as

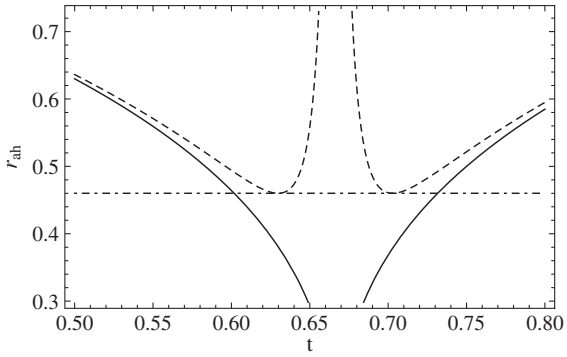

FIG. 3. The apparent horizon curve $r_{ah}(t)$ for the classical dust model (solid line) and the semiclassical model for $\gamma = 1$ (dashed line). If the boundary of the cloud is taken smaller than r_{min} (dashed-dotted line) there are never trapped surfaces forming in the quantum-inspired model. At the time of the bounce, when $\rho = \rho_{cr}$ and gravity is turned off, the spacetime is flat, and there is no horizon. This is a regime of asymptotic freedom.

$$M_{min} = 8\sqrt{\frac{a_{cr}^3}{27M_0}}. \tag{41}$$

From the above equation, we see that, if the critical density is taken of the order of the Planck density, then M_{min} must be very small.

In the more general case for larger collapsing objects, an apparent horizon forms at a time t a little bit later than the classical case. However, when the density ρ approaches the critical density ρ_{cr}, gravity becomes more and more weak (it is turned off completely when $\rho = \rho_{cr}$, which occurs at the time $t = t_{cr}$) and the spacetime reduces to the flat Minkowski case. The apparent horizon thus disappears (r_{ah} diverges) and the bounce is "immediately" visible to distant observers. Let us notice, however, that our model assumes a homogeneous density and therefore at the critical time t_{cr} gravity is turned off everywhere. In a more realistic scenario, where the density is higher at the center, the bounce may still be hidden behind a horizon produced by the matter at larger radii and lower densities. After the bounce, the collapse is reversed into an expansion and the matter density starts decreasing. As the asymptotic-freedom regime is left, gravity becomes strong again and a new apparent horizon forms. However, we are now in an expanding phase, and when the matter density becomes too low, the apparent horizon disappears forever. Since we are considering the marginally bound case, where collapse has zero velocity at spatial infinity, in the expanding phase the cloud will return to its initial configuration, but with positive velocity, and continue to expand until all the matter is radiated to infinity.

B. Quantum-inspired radiation model

Following what we did for the dust case, we turn now to the radiation collapse model, where the new scale function

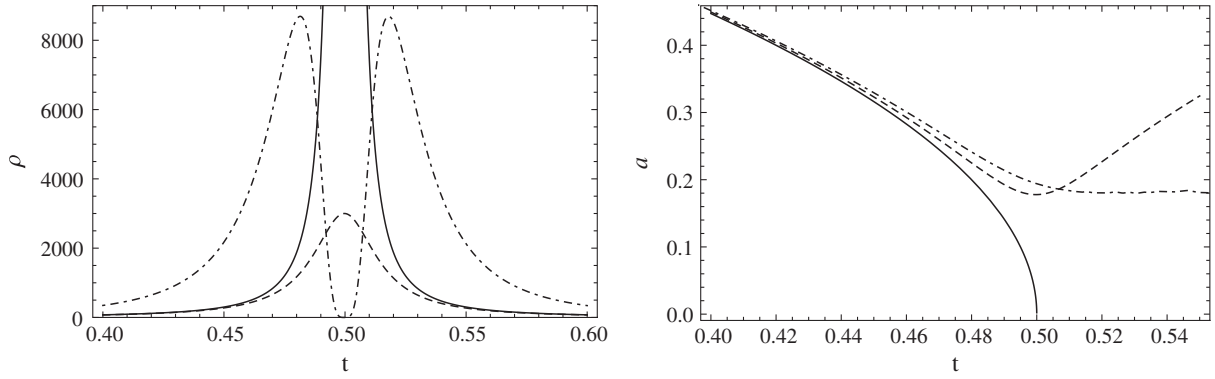

FIG. 4. Radiation collapse models. Left panel: The density ρ in the classical model (solid line), the density ρ in the quantum-inspired collapse model with $\gamma = 1$ (dashed line), and the effective density $\rho_{\rm eff}$ in the quantum-inspired collapse model with $\gamma = 1$ (dashed-dotted line). Right panel: Plot of $a(t)$ in the classical case (solid line) and in the semiclassical models with $\gamma = 1$ (dashed line) and $\gamma = 2$ (dotted-dashed line). Near the initial time, the semiclassical model has a behavior close to the classical radiation. a either reaches a minimum at $t = t_{\rm cr}$ and then grows for $t > t_{\rm cr}$ ($\gamma = 1$), or approaches asymptotically a minimum value ($\gamma = 2$). Here, $M_0 = 1$ and $\rho_{\rm cr} = 3000$. See the text for details.

a that appears in Eq. (20) has to be determined from the integration of the new equation of motion,

$$\dot{a}^2 = \frac{M_0}{a^2} + \alpha_1 \frac{3M_0^2}{a^6} + \alpha_2 \frac{9M_0^3}{a^{10}} + \cdots. \tag{42}$$

The effective density is again taken to be of the form given in Eq. (26) and the equation of motion becomes

$$\dot{a}^2 = \frac{M_0}{a^{4\gamma+2}}(a^4 - a_{\rm cr}^4)^\gamma, \quad \text{with} \quad a_{\rm cr}^4 = \frac{3M_0}{\rho_{\rm cr}}. \tag{43}$$

Solving the above equation in the two cases $\gamma = 1$ and 2, with the initial condition $a(0) = 1$, we obtain

$$t(a) = \frac{\sqrt{1 - a_{\rm cr}^4} - \sqrt{a^4 - a_{\rm cr}^4}}{2\sqrt{M_0}}, \quad \text{for } \gamma = 1, \tag{44}$$

$$t(a) = \frac{1 - a^2}{2\sqrt{M_0}} - \frac{a_{\rm cr}^2}{2\sqrt{M_0}}\left(\tanh^{-1}\left(\frac{1}{a_{\rm cr}^2}\right) - \tanh^{-1}\left(\frac{a^2}{a_{\rm cr}^2}\right)\right), \quad \text{for } \gamma = 2. \tag{45}$$

Once again, the two cases are substantially different since the scale function $a(t)$ reaches its minimum value $a_{\rm cr}$ in a finite time $t_{\rm cr}$ for $\gamma = 1$, while it needs an infinite time when $\gamma = 2$ (see the right panel in Fig. 4).

The effective pressure is still given by Eq. (30), where now we have the effective mass given by

$$M_{\rm eff} = \frac{M_0}{a}\left(1 - \frac{\rho}{\rho_{\rm cr}}\right)^\gamma. \tag{46}$$

The effective mass goes to zero as t approaches $t_{\rm cr}$, while the new mass for the radiation fluid, given by M_0/a, reaches a maximum value (see the left panel in Fig. 5). Evaluating the effective pressure, we find

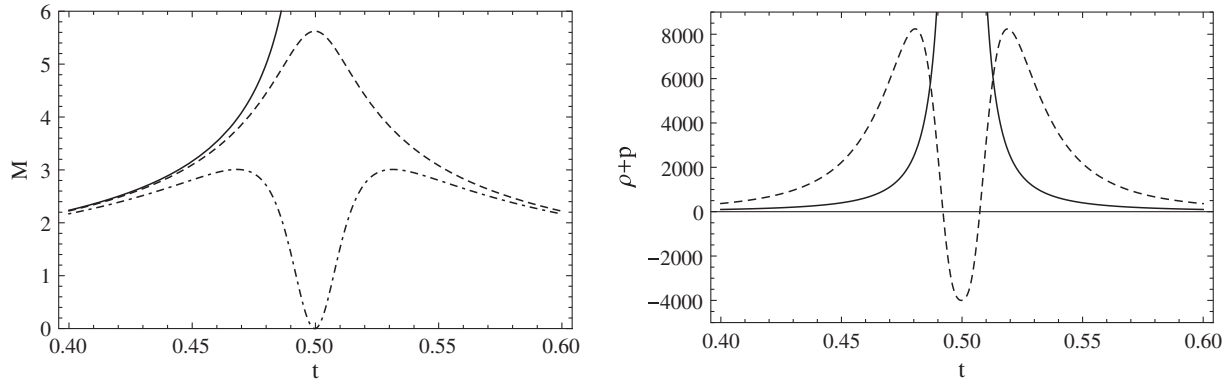

FIG. 5. Radiation collapse models. Left panel: The mass profile $M(t) = M_0/a$ for classical radiation (solid line) and for the semiclassical model (dashed line), together with the effective mass profile $M_{\rm eff}$ (dotted-dashed line). At $t = t_{\rm cr}$, in the semiclassical model $M(t)$ reaches a maximum, while the effective mass vanishes: the spacetime is flat and we are in a regime of asymptotic freedom. Right panel: $\rho + p$ for the classical radiation case (solid line) and $\rho_{\rm eff} + p_{\rm eff}$ for $\gamma = 1$ (dashed line). In the latter case, the weak energy condition does not hold in the strong-field limit. Here, $M_0 = 1$ and $\rho_{\rm cr} = 3000$. See the text for details.

$$p_{\rm eff} = \frac{\rho}{3}\left(1 - 5\gamma\frac{\rho}{\rho_{\rm cr}}\right)\left(1 - \frac{\rho}{\rho_{\rm cr}}\right)^{\gamma-1}. \quad (47)$$

In the strong-field region, the effective pressure becomes negative. In the case $\gamma = 1$, we see that $p_{\rm eff}$ becomes negative when the density reaches the value $\rho_{\rm cr}/5$, and it tends to $-4\rho/3$ in the limit of $\rho \to \rho_{\rm cr}$. In the case $\gamma = 2$, it becomes negative when the density is $\rho_{\rm cr}/10$, and then goes back to zero when ρ approaches $\rho_{\rm cr}$. The weak energy condition for the effective dynamics is given by $\rho_{\rm eff} + p_{\rm eff}$ and it is violated in the strong-field regime (see the right panel in Fig. 5).

We will now focus on the case $\gamma = 1$, for which the scale function becomes

$$a(t) = \left[a_{\rm cr}^4 + \left(\sqrt{1 - a_{\rm cr}^4} - 2\sqrt{M_0}t\right)^2\right]^{1/4}. \quad (48)$$

a reaches a minimum at $t_{\rm cr} < t_{\rm s}$, where $\dot{a}$ vanishes. At the critical time, the effective density goes to zero, while the new density reaches its maximum value $\rho_{\rm cr}$ (left panel in Fig. 4). Therefore the collapse is halted, originating a bounce.

Once again, an interesting question is what happens to the trapped surfaces in this context. In the classical case, one must choose the boundary such that $r_{\rm b} < 1/\sqrt{M_0}$ in order to avoid trapped surfaces at the initial time. In the semiclassical model, the condition becomes $r_{\rm b} < 1/\sqrt{M_0(1 - a_{\rm cr}^4)}$. The formation of trapped surfaces for the classical FRW radiation model is described by the time curve

$$t_{\rm ah}(r) = t_{\rm s} - \frac{r^2\sqrt{M_0}}{2}, \quad (49)$$

and the apparent horizon forms at the boundary of the cloud before the formation of the central singularity. In our quantum-inspired model, the apparent horizon curve is

$$r_{\rm ah}(t) = \frac{a^3}{\sqrt{M_0(a^4 - a_{\rm cr}^4)}}. \quad (50)$$

Like in the dust case, we can verify that there exists a minimum value $r_{\rm min}$, obtained as t goes to

$$t_{\rm min} = t_{\rm s}\left(\sqrt{1 - a_{\rm cr}^4} - \sqrt{2}a_{\rm cr}^2\right) \quad (51)$$

and it is given by

$$r_{\rm min} = r_{\rm ah}(t_{\rm min}) = 3^{3/4}\frac{a_{\rm cr}}{\sqrt{2M_0}}. \quad (52)$$

Therefore, if the boundary is taken so that $r_{\rm b} < r_{\rm min}$, no trapped surfaces form during the whole process of collapse and bounce (see Fig. 6). The existence of a minimum radius implies that there is a minimal mass $M_{\rm min}$ below which no apparent horizon can form. In the general case, like for the dust model, an apparent horizon forms at a time a little bit later than the classical prediction. It then disappears when the density approaches the critical value $\rho_{\rm cr}$ and the gravitational force is turned off ($r_{\rm ah}$ diverges). At the critical time, there is no horizon and the spacetime is flat. After the bounce, the density decreases and a new apparent horizon forms. The latter eventually disappears when the density becomes too low.

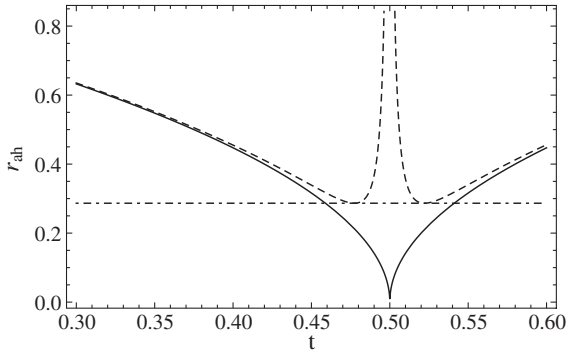

FIG. 6. The apparent horizon curve $r_{\rm ah}(t)$ for the classical radiation model (solid line) and the semiclassical model for $\gamma = 1$ (dashed line). If the boundary of the cloud is taken smaller that $r_{\rm min}$ (dashed-dotted line) there are no trapped surfaces forming in the quantum-inspired model. At the time of the bounce, when $\rho = \rho_{\rm cr}$ and gravity is turned off, the spacetime is flat and there is no horizon. This is a regime of asymptotic freedom.

IV. CONCLUDING REMARKS

Spacetime singularities, as obtained from exact solutions of Einstein's equations, are presumably the result of the breakdown of general relativity and they are supposed to be removed by quantum gravity corrections. So far, given the lack of a complete theory for quantum gravity, we do not really know how the issue of the formation of singularities is affected by quantum effects. It sounds plausible that singularities are bound to disappear once one treats the strong-field regime within a suitable quantum gravitational framework. Toy models like the one discussed in the present paper may suggest possible scenarios. Classical singularities in general relativity can either be covered by a horizon or be naked. The issue of whether naked singularities can occur in a physically realistic scenario is still an open problem. Nevertheless, an analysis that takes into account quantum effects when the gravitational field becomes sufficiently strong not only affects the formation of the singularity, but it also has an impact on the structure of trapped surfaces.

The main result of our work is that in our model the outcome of the gravitational collapse is not a black hole, in the sense of a region causally disconnected from future null infinity. While we have not explicitly verified if outgoing null geodesics launched from any point of the spacetime can propagate to null infinity, our results strongly suggest that this is indeed always the case. So there is no event horizon in these spacetimes and, in principle, the region

where Planck-scale effects become important could be visible to distant observers.

In our specific toy model with $\gamma = 1$, we found that a homogeneous collapsing object reaches a critical density. At this point, gravity is turned off and the apparent horizon disappears. After the bounce, gravity becomes strong again and a new apparent horizon forms. The picture does not seem to depend on the matter equation of state, and indeed we found the same result for dust and radiation. The case $\gamma = 2$ is qualitatively similar to the $\gamma = 1$ model for $t \leq t_{\rm cr}$, with $t_{\rm cr} \to \infty$; here there is no bounce and the asymptotic-freedom regime where gravity becomes weaker and weaker lasts for an infinite time, but gravity is never turned off, as the critical density is reached only in an infinite time.

Classical singularities arising in astrophysical scenarios and not covered by any horizon suggest the possibility of observing regions where Planck-scale physics produces detectable effects. This, in turn, may allow for the identification of a signature of quantum gravity and open the possibility of experimentally testing theories of quantum gravity via astrophysical observations. The long sought signature of quantum gravity, which has eluded any laboratory-based hunt, might then be found in catastrophic astrophysical events.

ACKNOWLEDGMENTS

This work was supported by the Thousand Young Talents Program and Fudan University.

[1] S. Tsujikawa, P. Singh, and R. Maartens, Classical Quantum Gravity **21**, 5767 (2004); M. Bojowald, G. Calcagni, and S. Tsujikawa, Phys. Rev. Lett. **107**, 211302 (2011); M. Bojowald, G. Calcagni, and S. Tsujikawa, J. Cosmol. Astropart. Phys. 11 (2011) 046.

[2] N. Arkani-Hamed, S. Dimopoulos, and G. R. Dvali, Phys. Lett. B **429**, 263 (1998); I. Antoniadis, N. Arkani-Hamed, S. Dimopoulos, and G. R. Dvali, Phys. Lett. B **436**, 257 (1998).

[3] G. Amelino-Camelia, J. R. Ellis, N. E. Mavromatos, D. V. Nanopoulos, and S. Sarkar, Nature (London) **393**, 763 (1998).

[4] R. Penrose, Riv. Nuovo Cimento **1**, 252 (1969); Gen. Relativ. Gravit. **34**, 1141 (2002).

[5] D. M. Eardley and L. Smarr, Phys. Rev. D **19**, 2239 (1979); D. Christodoulou, Commun. Math. Phys. **93**, 171 (1984); R. P. A. C. Newman, Classical Quantum Gravity **3**, 527 (1986); B. Waugh and K. Lake, Phys. Rev. D **38**, 1315 (1988); G. Magli, Classical Quantum Gravity **14**, 1937 (1997); **15**, 3215 (1998); T. Harada, K. I. Nakao, and H. Iguchi, Classical Quantum Gravity **16**, 2785 (1999); T. Harada and H. Maeda, Phys. Rev. D **63**, 084022 (2001); R. Goswami and P. S. Joshi, Classical Quantum Gravity **19**, 5229 (2002); R. Giambò, F. Giannoni, G. Magli, and P. Piccione, Commun. Math. Phys. **235**, 545 (2003); R. Goswami and P. S. Joshi, Phys. Rev. D **69**, 044002 (2004); R. Giambò, J. Math. Phys. (N.Y.) **47**, 022501 (2006); P. S. Joshi, D. Malafarina, and R. V. Saraykar, Int. J. Mod. Phys. D **21**, 1250066 (2012).

[6] P. S. Joshi and D. Malafarina, Int. J. Mod. Phys. D **20**, 2641 (2011).

[7] Z. Li and C. Bambi, Phys. Rev. D **87**, 124022 (2013).

[8] C. Bambi and K. Freese, Phys. Rev. D **79**, 043002 (2009); C. Bambi, K. Freese, T. Harada, R. Takahashi, and N. Yoshida, Phys. Rev. D **80**, 104023 (2009); C. Bambi, T. Harada, R. Takahashi, and N. Yoshida, Phys. Rev. D **81**, 104004 (2010); C. Bambi and N. Yoshida, Classical Quantum Gravity **27**, 205006 (2010); C. Bambi, Europhys. Lett. 94, 50002 (2011); J. Cosmol. Astropart. Phys. 05 (2011) 009; C. Bambi, F. Caravelli, and L. Modesto, Phys. Lett. B **711**, 10 (2012); Z. Li and C. Bambi, J. Cosmol. Astropart. Phys. 03 (2013) 031; C. Bambi and D. Malafarina, arXiv:1307.2106 [Phys. Rev. D (to be published)]; A. N. Chowdhury, M. Patil, D. Malafarina, and P. S. Joshi, Phys. Rev. D **85**, 104031 (2012); P. S. Joshi, D. Malafarina, and R. Narayan, Classical Quantum Gravity **28**, 235018 (2011); D. Pugliese, H. Quevedo, and R. Ruffini, Phys. Rev. D **84**, 044030 (2011); **83**, 104052 (2011); Z. Kovacs and T. Harko, Phys. Rev. D **82**, 124047 (2010); K. S. Virbhadra and G. F. R. Ellis, Phys. Rev. D **65**, 10300 (2002).

[9] L. Modesto, J. W. Moffat, and P. Nicolini, Phys. Lett. B **695**, 397 (2011); L. Modesto, Phys. Rev. D **86**, 044005 (2012); arXiv:1202.3151 [Astron. Rev. (to be published)].

[10] L. Modesto, Int. J. Theor. Phys. **45**, 2235 (2006); Classical Quantum Gravity **23**, 5587 (2006); P. Nicolini, A. Smailagic, and E. Spallucci, Phys. Lett. B **632**, 547 (2006); L. Modesto, Int. J. Theor. Phys. **47**, 357 (2008); Adv. High Energy Phys. **2008**, 459290 (2008); P. Nicolini, Int. J. Mod. Phys. A **24**, 1229 (2009); L. Modesto and I. Premont-Schwarz, Phys. Rev. D **80**, 064041 (2009); S. Hossenfelder, L. Modesto, and I. Premont-Schwarz, Phys. Rev. D **81**, 044036 (2010); L. Modesto, Int. J. Theor. Phys. **49**, 1649 (2010); L. Modesto and P. Nicolini, Phys. Rev. D **82**, 104035 (2010).

[11] M. Bojowald, Phys. Rev. Lett. **86**, 5227 (2001); A. Ashtekar, T. Pawlowski, and P. Singh, Phys. Rev. D **73**, 124038 (2006); **74**, 084003 (2006); E. Wilson-Ewing, J. Cosmol. Astropart. Phys. 03 (2013) 026.

[12] M. Bojowald, R. Goswami, R. Maartens, and P. Singh, Phys. Rev. Lett. **95**, 091302 (2005); R. Goswami, P. S. Joshi, and P. Singh, Phys. Rev. Lett. **96**, 031302 (2006); R. Casadio, S. D. H. Hsu, and B. Mirza, Phys. Lett. B **695**, 317 (2011).

[13] Y. Tavakoli, J. Marto, and A. Dapor, arXiv:1303.6157.

[14] J. R. Oppenheimer and H. Snyder, Phys. Rev. **56**, 455 (1939).

[15] C. Barcelo and M. Visser, Int. J. Mod. Phys. D **11**, 1553 (2002); P. Martin-Moruno and M. Visser, arXiv:1305.1993 [Phys. Rev. Lett. (to be published)].

[16] G. Lemaître, Annales Soc. Sci. Brux. Ser. I Sci. Math. Astron. Phys. A **53**, 51 (1933); Gen. Relativ. Gravit. **29**, 641 (1997); R. C. Tolman, Proc. Natl. Acad. Sci. U.S.A. **20**, 169 (1934); Gen. Relativ. Gravit. **29**, 935 (1997); H. Bondi, Mon. Not. R. Astron. Soc. **107**, 410 (1947).

[17] W. Israel, Nuovo Cimento B **44**, 1 (1966); **48**, 463(E) (1967); P. S. Joshi and I. H. Dwivedi, Classical Quantum Gravity **16**, 41 (1999); R. Giambò, Classical Quantum Gravity **22**, 2295 (2005).

[18] P. S. Joshi and I. H. Dwivedi, Phys. Rev. D **47**, 5357 (1993); P. S. Joshi, N. Dadhich, and R. Maartens, Phys. Rev. D **65**, 101501 (2002).

[19] N. O. Santos, Mon. Not. R. Astron. Soc. **216**, 403 (1985).

[20] R. Goswami, P. S. Joshi, C. Vaz, and L. Witten, Phys. Rev. D **70**, 084038 (2004); M. Patil, P. S. Joshi, and D. Malafarina, Phys. Rev. D **83**, 064007 (2011).